

Calculations of Undulator Radiation

Lewis Kotredes

*Physics Department, Worcester Polytechnic Institute
Worcester, MA, 01609*

Abstract

A brief description of undulator radiation and its uses is followed by derivations of several forms for an equation governing the Fourier transform of the electric field from electrons in an undulator. Aspects of the derivation are discussed, and a number of graphs comparing the forms with each other and with other work are presented. A graph of radiation through a monochromator is shown to agree well with work done by scientists at the ESRF.

Introduction

Since their discovery by Roentgen in the early twentieth century, x-rays have been used for many things. Due to their high photon energy and corresponding short wavelength, they are commonly used to examine the atomic structure of matter and learn details about its composition. Despite this usefulness, however, x-rays are extremely difficult to generate and control. One method, which has been implemented at a number of high energy particle sources around the world, including the CHESS facility at Cornell, is through the use of synchrotron radiation as an x-ray source.

Synchrotron radiation is a good x-ray source, but for studies of matter you want as bright a beam as can be attained. This can be achieved through the use of wiggler and undulator magnets. These devices generally consist of alternating north-south dipole magnets aligned along the track of a particle, often an electron (or an electron beam). These magnets cause the electrons to move in an approximately sinusoidal fashion, and thus cause them to emit x-rays. These x-ray photons typically lie within a very small cone of the direction of motion, and thus tend to be very bright.

This paper will discuss a treatment of undulator and wiggler radiation, using both a numerical integration and an analytic form of the same equation evaluated using Anger and Weber functions. These functions are related to Bessel functions, and can be used to express our solution in a series expansion. In addition, they are known to MAPLE, a standard mathematical program, and as such can be effectively used to effect calculations more rapidly than the integral form they approximate. Some calculations using these forms will also be compared to published results, especially some results produced at the ESRF accelerator in France, and will be shown to agree very well with these results.

Undulator Radiation as an Integral

Radiation from an undulator magnet can be well treated using techniques similar to those used for discussions of synchrotron radiation (see Hofmann [1]). As already stated, an undulator magnet consists of a series of alternating north and south pole magnets along the axis of an electron's path. The main difference between undulators and simple synchrotron radiation is the fact that the alternating poles act to keep the electron moving within a

roughly linear path. This means that the x-rays, as opposed to being tangential to a circle by the movement of the electrons, are directed within a tight cone for a considerable time, compared with that obtained in a synchrotron. In addition, the alternating poles will lead to an interference condition similar to that seen in a diffraction grating (which will be a useful analogy in understanding the radiation distributions).

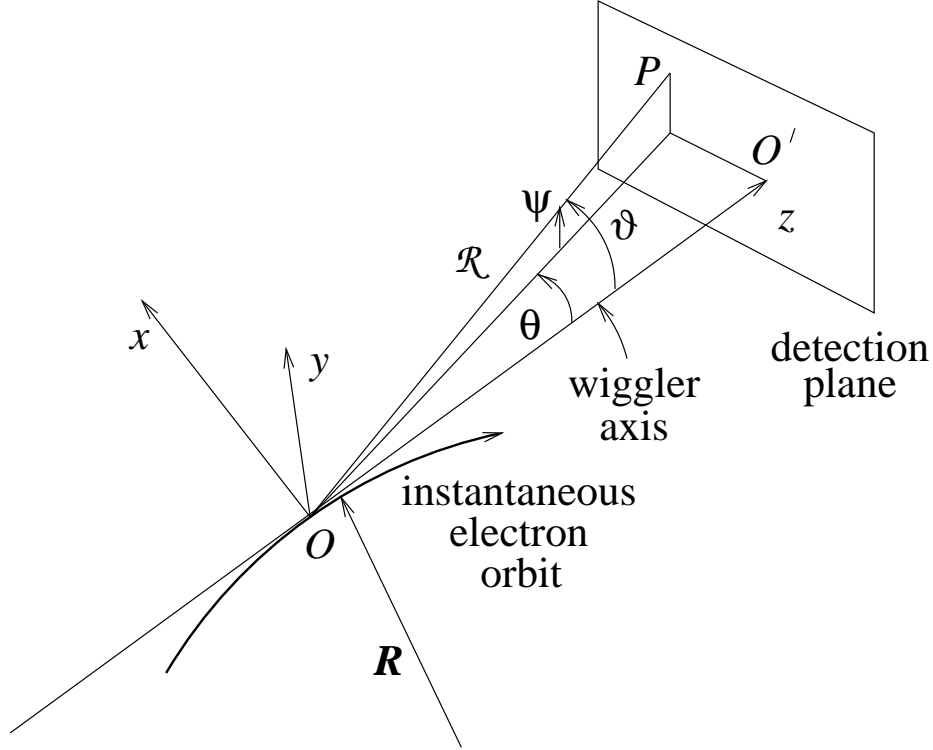


FIGURE 1. This diagram shows the angular definitions used in this paper

The defining equation for the electric field from the undulator is given by the well-known Liénard-Wiechert equation for the radiation term of the \mathbf{E} field from a moving point charge.

$$\mathbf{E}(t) = \frac{q}{4\pi c\epsilon_0} \left(\frac{\hat{\mathcal{R}} \times [(\hat{\mathcal{R}} - \beta) \times \dot{\beta}]}{\mathcal{R}(1 - \hat{\mathcal{R}} \cdot \beta)^3} \right)_{ret}. \quad (1)$$

However, we shall (following Talman [3]) immediately use a Fourier transform, and in so doing we obtain:

$$\tilde{\mathbf{E}}(\omega) = \frac{q}{4\pi\epsilon_0 c\mathcal{R}} \frac{1}{\sqrt{2\pi}} \int_{-\infty}^{\infty} e^{i\omega t} \left(\frac{[\hat{\mathcal{R}} \times [(\hat{\mathcal{R}} - \beta) \times \dot{\beta}]]}{\mathcal{R}(1 - \hat{\mathcal{R}} \cdot \beta)^3} \right)_{ret} dt \quad (2)$$

This can, after a change to the variable of integration and an integration by parts, be changed to

$$\tilde{\mathbf{E}}(\omega, \theta, \psi) = \frac{q}{4\pi\epsilon_0 c\mathcal{R}} \frac{i\omega}{\sqrt{2\pi}} \int_{-\infty}^{\infty} e^{i\omega t(t_r)} \frac{\mathbf{v}_{\perp}}{c} dt_r \quad (3)$$

where \mathbf{v}_{\perp} is the perpendicular component of the velocity relative to the radius from the particle to the observation point and t_r is the retarded time at the point of observation. The

value of \mathbf{v}_\perp , by geometry, can be shown to be, assuming θ and ψ are small,

$$\frac{\mathbf{v}_\perp}{c} \approx \begin{pmatrix} \Theta \cos(k_w z) - \theta \\ -\psi \end{pmatrix} \quad (4)$$

Note here that the z-component of \mathbf{v}_\perp is assumed to be small compared to other terms and is neglected; $k_w = 2\pi/\lambda_w$, where λ_w is the distance between undulator poles, and $\Theta = K/\gamma$, where K is an undulator parameter defined such that Θ is the angle between the electron path and the axis. Also, this expression for \mathbf{v}_\perp is valid only within the range of time where the electron is inside the undulator; outside of this range it is taken to be zero. Substituting Eq. (4) into Eq. (3), and again making some substitutions, we obtain

$$\frac{\tilde{\mathbf{E}}(\omega, \theta, \psi)}{\frac{q}{4\pi\epsilon_0 c \mathcal{R}}} = \frac{i\omega}{\sqrt{2\pi}} \frac{1}{k_w c} \int_{-\pi}^{(2N_w-1)\pi} \exp\left(i \frac{\omega}{\omega_1(\vartheta)} \phi_t(\phi_z)\right) \begin{pmatrix} \Theta \cos \phi_z - \theta \\ -\psi \end{pmatrix} d\phi_z \quad (5)$$

The reason for the apparently odd choice of bounds on the integral will become clearer. The following substitutions were made in deriving Eq. (5):

$$\begin{aligned} \omega_1(\vartheta) &= \frac{2\gamma^2}{1 + K^2/2 + \gamma^2\vartheta^2} c k_w, \quad \vartheta^2 = \theta^2 + \psi^2, \quad \phi_z = k_w z \\ \phi_t(\phi_z) &= \phi_z + p \sin \phi_z + q \sin 2\phi_z. \\ p &= -\frac{2\gamma\theta K}{1 + K^2/2 + \gamma^2\theta^2} \quad q = \frac{K^2/4}{1 + K^2/2 + \gamma^2\theta^2} \end{aligned}$$

You should note that ω_1 is a function of the angular position of the observer. As the name implies, ω_1 is a baseline frequency that has special significance; the fact that it varies with angular position is worth keeping in mind. A specific case this applies to is when one looks at the spectrum through a monochromator, which will select only x-rays of a given frequency.

Now, Eq. (5) is a relatively simple integral that can be evaluated in terms of θ , ψ , and ω for a given undulator. However, it can be simplified yet further by examining the integral closely. Specifically, the integrand is such that an advancement by 2π in ϕ_z will result only in a net multiplication by a phasor factor

$$\exp\left(2i\pi \frac{\omega}{\omega_1}\right).$$

Thus, the integral can be broken down into a sum of integrals, each different by only a phasor factor. We can sum these phasor factors outside of the integral, which will itself be evaluated only between the bounds $-\pi$ and π . It is this integral, over the diminished range, that will prove to be expandable in terms of the Anger and Weber functions.

Summation of the phasor factors yields a very useful result, which will help explain some important properties of the undulator. This summation has the form of a simple geometric series that can be evaluated to

$$\sum_{j=0}^{N_w-1} \exp\left(2i\pi \frac{\omega}{\omega_1} j\right) = \frac{1 - \exp\left(2\pi i \frac{\omega}{\omega_1} N_w\right)}{1 - \exp\left(2\pi i \frac{\omega}{\omega_1}\right)} \quad (6)$$

$$= e^{\pi i \frac{\omega}{\omega_1} (N_w-1)} \frac{\sin\left(\pi \frac{\omega}{\omega_1} N_w\right)}{\sin\left(\pi \frac{\omega}{\omega_1}\right)}. \quad (7)$$

Note the complex exponential term that begins the right-hand side of this equation. This term has a magnitude of 1, and is a function to the distance between our zero point and the center of the integral; in measuring (say) intensity, you will have to calculate the absolute square of $\tilde{\mathbf{E}}$. In this case, the complex exponential phase factor will disappear, so we are left with the important part of the phasor sum being only

$$\frac{\sin\left(\pi\frac{\omega}{\omega_1}N_w\right)}{\sin\left(\pi\frac{\omega}{\omega_1}\right)}, \quad (8)$$

which will hereafter be referred to as the “phasor sum”. Notice that this phasor sum has a limiting condition; as the ratio ω/ω_1 approaches an integer value, this sum will go to the value N_w . At other times it has a range of values, but they fall off quickly to any side of the harmonic and typically evaluate to a value much less than the value obtained in the harmonic condition. This means that for an undulator with many periods, the magnitude of $\tilde{\mathbf{E}}$ will be much greater when the radiation is on a harmonic of $\omega_1(\vartheta)$ than when it is not; ultimately, the off-harmonic radiation is very nearly negligible when compared to that on harmonics. Indeed, since intensity is related to the square of $\tilde{\mathbf{E}}$, the effect is even more pronounced when measuring intensity, which is often the interest in practice.

The integral itself, evaluated only from $-\pi$ to π , can be simplified yet once more. This integral is being evaluated over a symmetric domain; we can divide the complex exponential into real and imaginary parts. When we do so, we find that the cosine (real) term is even, it can be simplified to an integral from 0 to π . The sine term, on the other hand, is odd and vanishes. Substituting for $\omega/\omega_1(\vartheta)$ the dimensionless η and simplifying all terms, we obtain our integral form for the Fourier transforms (leaving off as unimportant phasor factors and multiples of i):

$$\frac{\tilde{E}_x(\omega, \theta, \psi)}{\frac{q}{4\pi\epsilon_0 c \mathcal{R}}} = \frac{\sin(\pi\eta N_w)}{\sin(\pi\eta)} \sqrt{\frac{2}{\pi}} \frac{\omega}{k_w c} \int_0^\pi \cos(\eta\phi_t(\phi_z)) (\Theta \cos\phi_z - \theta) d\phi_z \quad (9)$$

$$\frac{\tilde{E}_y(\omega, \theta, \psi)}{\frac{q}{4\pi\epsilon_0 c \mathcal{R}}} = \frac{\sin(\pi\eta N_w)}{\sin(\pi\eta)} \sqrt{\frac{2}{\pi}} \frac{\omega}{k_w c} \int_0^\pi \cos(\eta\phi_t(\phi_z)) (-\psi) d\phi_z \quad (10)$$

Undulator Radiation in an Analytic Form

Evaluation of this integral form is a fairly straightforward task using MAPLE or other mathematical programs. However, although the calculations themselves can be easily set up, their execution requires considerable computer time. What would be preferable would be an expression for this integral that could be evaluated, instead of by repeating a numerical integration, by looking at tables or otherwise simpler methods. This section follows the method outlined in Talman [4]. To this end, we can examine the term $\cos(\eta(\phi_z + p \sin(\phi_z) + q \sin(2\phi_z)))$, which you will recognize as $\cos(\phi_t(\phi_z))$. Using the angle addition formula for cosine, we break this up into two terms:

$$\begin{aligned} \cos(\eta\phi_z + \eta p \sin(\phi_z) + \eta q \sin(2\phi_z)) &= \cos(\eta\phi_z + \eta q \sin(2\phi_z)) \cos(\eta p \sin(\phi_z)) \quad (11) \\ &+ \sin(\eta\phi_z + \eta q \sin(2\phi_z)) \sin(\eta p \sin(\phi_z)). \end{aligned}$$

These terms each contain a trigonometric function with argument $\eta p \sin(\phi_z)$. Those functions can be expanded by a Taylor series, in which we shall have i_{max} terms. Each expansion, then, will include terms with powers of sine, which can be put into a new form by expanding these powers in terms of $\cos(j\phi_z)$ and $\sin(j\phi_z)$. It should be noted that expansions of $\sin^n \phi_z$ will yield only $\cos(j\phi_z)$ terms if n is even and $\sin(j\phi_z)$ terms if n is odd. Using this property, we recognize that

$$\begin{aligned} I_{C,j} &= \int_0^\pi \cos(\eta(\phi_z + q \cos 2\phi_z)) \cos(j\phi_z) d\phi_z \\ &= \frac{1}{4} \int_0^{2\pi} \cos\left(\frac{\eta-j}{2}\xi + \eta q \sin \xi\right) d\xi + \frac{1}{4} \int_0^{2\pi} \cos\left(\frac{\eta+j}{2}\xi + \eta q \sin \xi\right) d\xi \end{aligned} \quad (12)$$

$$\begin{aligned} I_{S,j} &= \int_0^\pi \sin(\eta(\phi_z + q \cos 2\phi_z)) \sin(j\phi_z) d\phi_z \\ &= \frac{1}{4} \int_0^{2\pi} \cos\left(\frac{\eta-j}{2}\xi + \eta q \sin \xi\right) d\xi - \frac{1}{4} \int_0^{2\pi} \cos\left(\frac{\eta+j}{2}\xi + \eta q \sin \xi\right) d\xi, \end{aligned} \quad (13)$$

after some trigonometry and a change of integration variable. Note the indexing in terms of j ; the final form that will be obtained is in the form of a series of summations. These integrals, however, can be expressed succinctly in terms of Anger and Weber functions. These functions are defined by

$$\text{Anger: } \pi \mathbf{J}_\mu = \int_0^\pi \cos(\mu\theta - z \sin \theta) d\theta \quad (14)$$

$$\text{Weber: } \pi \mathbf{E}_\mu = \int_0^\pi \sin(\mu\theta - z \sin \theta) d\theta \quad (15)$$

Thus, the integrals above can be changed into Anger and Weber functions; see Watson [5] for methodology. Doing so, we obtain

$$\begin{aligned} I_{C,j} &= \frac{\pi}{2} \cos^2\left(\frac{\eta-j}{2}\pi\right) \mathbf{J}_{\frac{\eta-j}{2}}(-\eta q) + \frac{\pi}{4} \sin((\eta-j)\pi) \mathbf{E}_{\frac{\eta-j}{2}}(-\eta q) \\ &\quad + \frac{\pi}{2} \cos^2\left(\frac{\eta+j}{2}\pi\right) \mathbf{J}_{\frac{\eta+j}{2}}(-\eta q) + \frac{\pi}{4} \sin((\eta+j)\pi) \mathbf{E}_{\frac{\eta+j}{2}}(-\eta q) \end{aligned} \quad (16)$$

$$\begin{aligned} I_{S,j} &= \frac{\pi}{2} \cos^2\left(\frac{\eta-j}{2}\pi\right) \mathbf{J}_{\frac{\eta-j}{2}}(-\eta q) + \frac{\pi}{4} \sin((\eta-j)\pi) \mathbf{E}_{\frac{\eta-j}{2}}(-\eta q) \\ &\quad - \frac{\pi}{2} \cos^2\left(\frac{\eta+j}{2}\pi\right) \mathbf{J}_{\frac{\eta+j}{2}}(-\eta q) - \frac{\pi}{4} \sin((\eta+j)\pi) \mathbf{E}_{\frac{\eta+j}{2}}(-\eta q). \end{aligned} \quad (17)$$

As you may have noticed, the expansion of the powers of sine yield not only sine terms, but also coefficients. These coefficients can be expressed in terms of a binomial expansion. If you combine coefficients from the expansion of the powers of sine with the coefficients from the Taylor series itself, you obtain

$$\begin{aligned} f(m, j) &= \frac{\text{binomial}(m, (m-j)/2)}{m! 2^{(m-1)}} \\ a(\eta, j) &= (-1)^{j/2} \sum_{i=0}^{i_{max}} (-1)^i (\eta p)^{2i} f(2i, j), \end{aligned} \quad (18)$$

$$b(\eta, j) = (-1)^{(j-1)/2} \sum_{i=0}^{i_{max}} (-1)^i (\eta p)^{(2i+1)} f(2i+1, j). \quad (19)$$

Now, the a coefficients are going to be used with the $I_{C,j}$ and are so defined only when j is even; by the same token, the b coefficients are used with the $I_{S,j}$ and are defined when j is odd. The last complication is the $\Theta \cos \phi_z$ term that appears in the expression for \tilde{E}_x . This term can be multiplied into the other cosine or sine terms when defining $I_{C,j}$ or $I_{S,j}$. When this happens, you obtain

$$\frac{1}{2}I_{C,j+1} + \frac{1}{2}I_{C,j-1}$$

or the same thing in terms of sines instead. Lastly, the coefficient for $I_{C,0}$ is unusual because of a factor of $1/2$ that appeared in the sine power expansion. When all is said and done, you will obtain for $\tilde{\mathbf{E}}$

$$\begin{aligned} \frac{\gamma \tilde{E}_x}{\frac{q}{4\pi\epsilon_0 c \mathcal{R}}} &= \frac{\eta \omega_1(\vartheta)}{k_w c} \sqrt{\frac{2}{\pi}} \left(\frac{K}{2} \left(\sum_{i'=0}^{i_{max}-1} (a(\eta, 2i') + a(\eta, 2i' + 2)) I_{C,2i'+1} + a(\eta, 2i_{max}) I_{C,2i_{max}+1} \right) \right) \\ &- \frac{K}{2} \left(\sum_{i'=0}^{i_{max}-1} (b(\eta, 2i' + 1) + b(\eta, 2i' + 3)) I_{S,2i'+2} + b(\eta, 2i_{max} + 1) I_{S,2i_{max}+2} \right) \\ &- \left(\gamma \theta \left(\frac{a(\eta, 0)}{2} I_{C,0} + \sum_{i'=1}^{i_{max}} a(\eta, 2i') I_{C,2i'} - \sum_{i'=0}^{i_{max}} b(\eta, 2i' + 1) I_{S,2i'+1} \right) \right) \end{aligned} \quad (20)$$

$$\frac{\gamma \tilde{E}_y}{\frac{q}{4\pi\epsilon_0 c \mathcal{R}}} = \frac{\eta \omega_1(\vartheta)}{k_w c} \sqrt{\frac{2}{\pi}} (-\gamma \psi) \left(\frac{a(\eta, 0)}{2} I_{C,0} + \sum_{i'=1}^{i_{max}} a(\eta, 2i') I_{C,2i'} - \sum_{i'=0}^{i_{max}} b(\eta, 2i' + 1) I_{S,2i'+1} \right) \quad (21)$$

This form appears fairly complicated, but it generally computes (for a reasonable value of i_{max} , typically on the order of 15 or so) much more quickly than the integral formulation on MAPLE.

Some Comments on Undulator Radiation

A careful examination of the equation for $\tilde{\mathbf{E}}$ yields useful insights. If one looks at the analytic form for $\tilde{\mathbf{E}}$, you may notice that the equations depend on $\gamma\theta$ and $\gamma\psi$, but not θ or ψ on their own. This can be usefully interpreted to mean that if one changes the value of γ , the angular pattern of the radiation will not change. Instead, the pattern will maintain its form while it shrinks into a smaller and smaller cone as γ increases. At the same time, however, the intensities within this cone will increase as γ^2 (note the hidden factor of γ^2 in ω_1). In this, however, the area over which this intensity is spread is decreasing by the same factor. The total energy radiated, however, goes as γ^2 . This factor comes from the fact that the energy inherent in the frequency of the radiation is also going as γ^2 , due to the same dependence of ω_1 on γ in the numerator.

Another important thing to notice is the way in which the radiation changes as K changes. At low values of K , the spectrum is almost entirely composed of the first harmonic. As K increases, however, the spectrum becomes, in a sense, dirtier. Other harmonics start appearing, first the third, then the fifth, and so on. On axis the odd harmonics will become as intense, and eventually more intense, than the fundamental. To demonstrate this, see Figure 2, which examines the value of $\tilde{\mathbf{E}}^2$ on axis for the first, third, fifth, seventh, and ninth

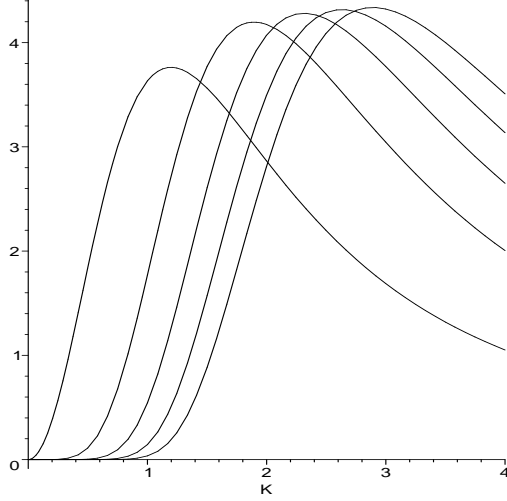


FIGURE 2. This graph, which also appears in Kim [2], shows how intensity on axis varies with K

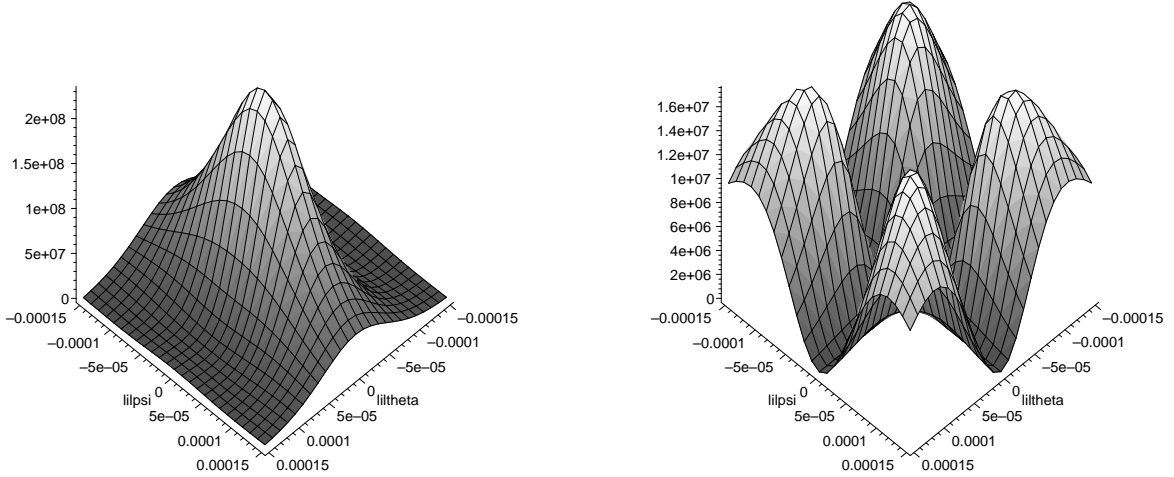


FIGURE 3. This pair of graphs shows the first harmonic; the left graph shows the x-polarization and the right the y-polarization. Bounds are $-1.5/\gamma$ to $1.5/\gamma$

harmonics (in order from left to right of peaks).

Calculated Results and Comparisons

Naturally, with a pair of forms for the equation for $\tilde{\mathbf{E}}$ some comparisons were required, both to check the accuracy of the analytic form as regards the integral form, and also to compare both to published profiles. Graphs in this section were produced using MAPLE.

The first comparison was between profiles for $|\tilde{\mathbf{E}}|^2$ in both x- and y-polarizations for the first harmonic ($\eta = 1$). These profiles are well known and appear in a number of standard texts on undulators, including Hofmann [1]. We also compared profiles for the second and third harmonics with those in Kim [2]: both of these agreed very well with the published profiles.

Although our formula should be equally valid for off-harmonic measurements as for those on a harmonic, we could not confirm this against any published profiles, due to a lack thereof.

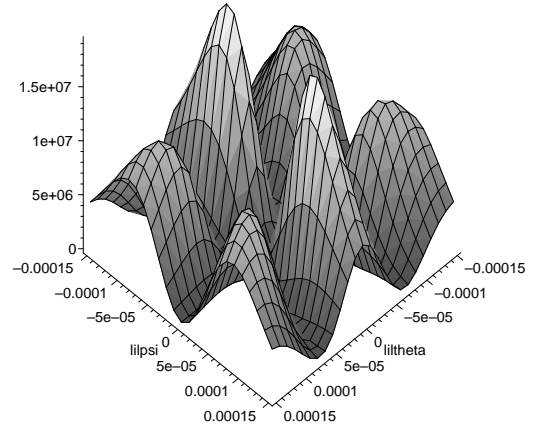
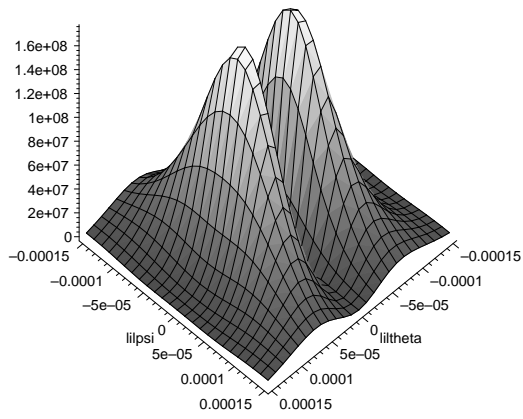


FIGURE 4. Same as Figure 3, for the second harmonic. Note that vertical scales are internally consistent for Figures 3, 4, and 5

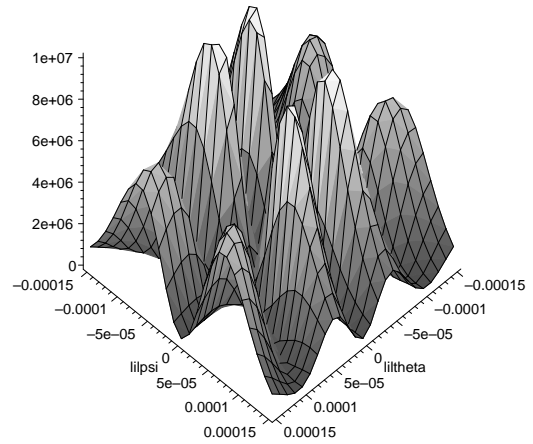
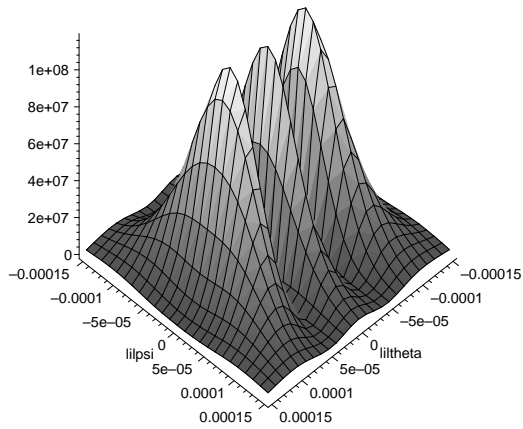


FIGURE 5. Same as Figures 3 and 4, for the third harmonic

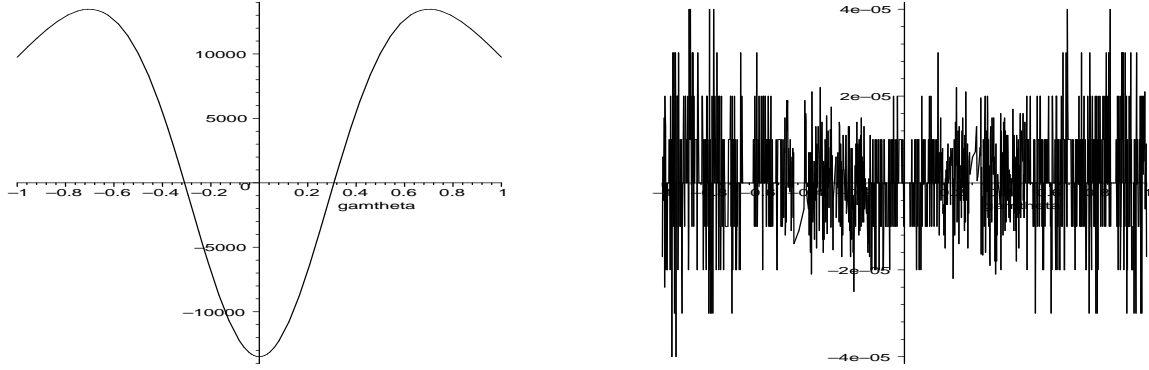


FIGURE 6. The left of these two graphs is a cross-section of the third harmonic, taken off-axis, calculated using both integral and analytic forms; the right is a plot of the difference of the two

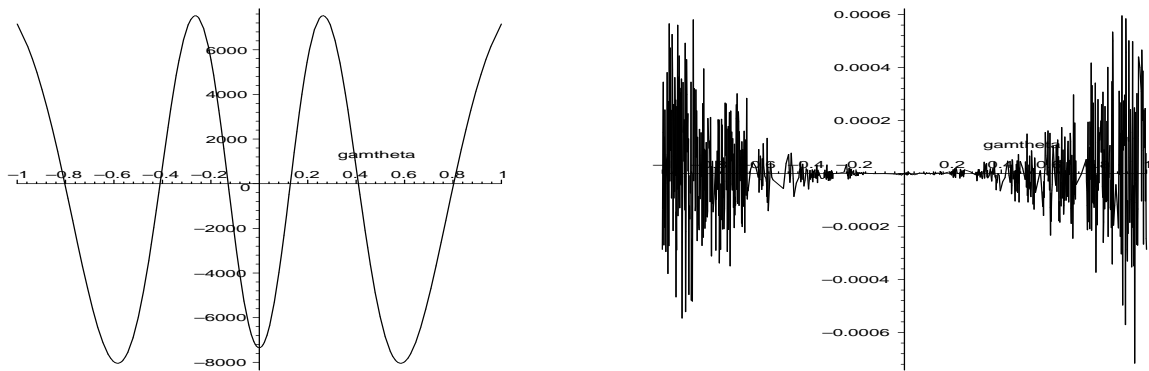


FIGURE 7. Same as Figure 6, except that this one represents the 7th harmonic

As was discussed in the section on the integral form of $\tilde{\mathbf{E}}$, the phasor sum tends to accentuate the radiation on the harmonics while leaving off-harmonic measurements relatively weak. Thus, from an undulator with any reasonably large number of periods the off-harmonic radiation is going to be all but unnoticeable.

Another important comparison is between the integral and analytic forms of $\tilde{\mathbf{E}}$. The analytic form is much quicker to calculate, as a rule, than the integral form, but this would be unimportant if the analytic form differed from the integral form. It should be noted that, if you use less terms, the formulae will agree well at first and then begin to diverge, with the

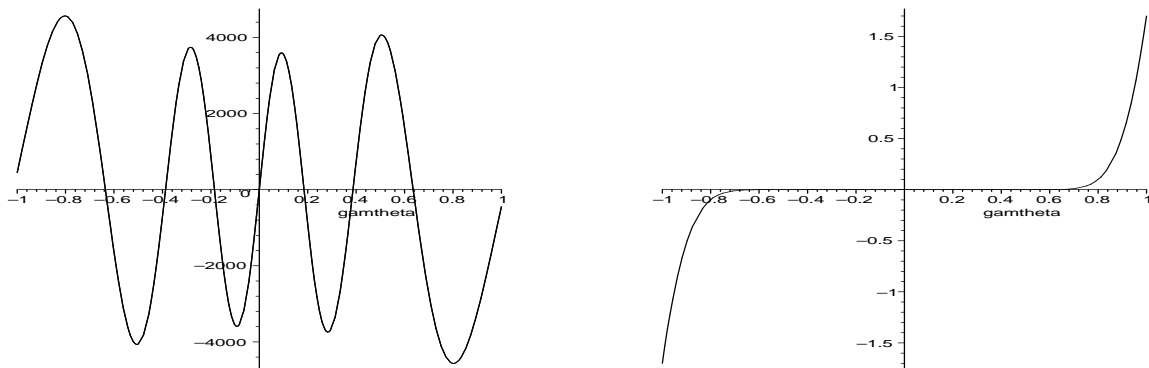


FIGURE 8. Same as figures 6 and 7, for the 10th harmonic

analytic form going to infinity. Using a value of $i_{max} = 14$, we took cross-sectional slices of the radiation profile for a given harmonic at a given value of ψ (we left ψ constant and varied θ) and compared them. The next several figures are paired, with the first figure showing a superposition of the two curves on the same graph, and the second the results obtained by taking the difference of the values at various points. As you can see, the error is negligible on the scale of the radiation.

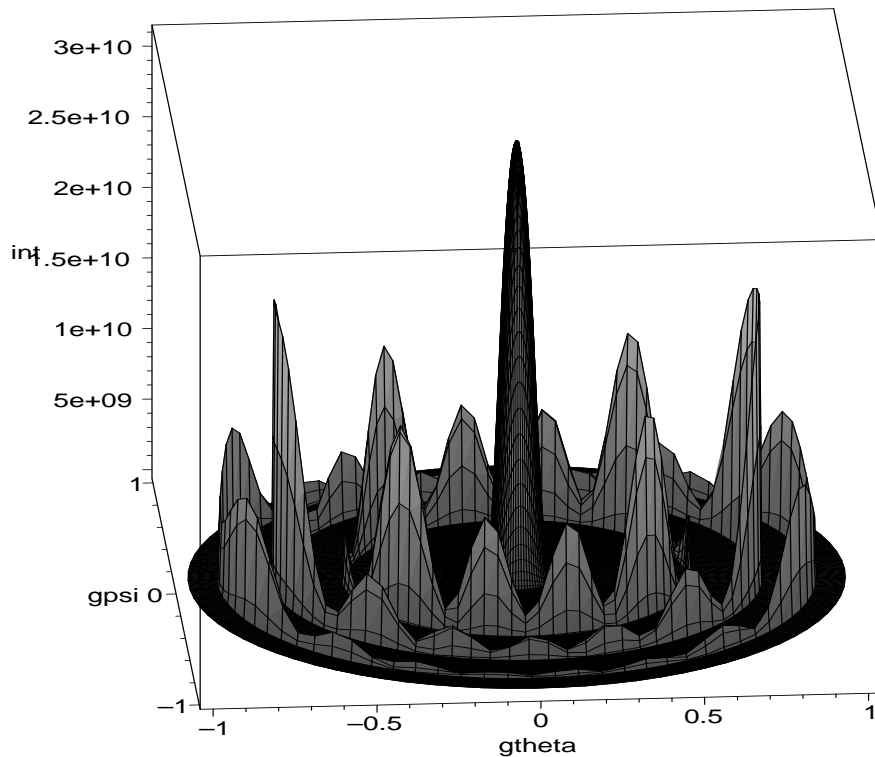


FIGURE 9. This is the ESRF graph we produced on MAPLE, a measure of intensity against $\gamma\theta$ (gtheta) and $\gamma\psi$ (gpsi). Compare this to the profile located on the ESRF web page, at <http://www.esrf.fr/machine/support/ids/Public/CentralCone/CentralCone.html>

The last comparison is the most ambitious. We duplicated the stated conditions for the profile for radiation in a graph on the ESRF website, and attempted to duplicate their results using our method. The following 3-D plot shows our results. These correspond well to the results on the ESRF webpage. A few comments are in order. First, due to our execution of the graphing, a small radiation peak that is visible on the ESRF graph that is not present in ours. This is not due to a mistake in the analytic form of the function. Rather, it is due to our method of solving the problem; to reduce the computation time necessary, the value of the function was not evaluated if η exceeded a certain distance from a harmonic, where the phasor sum would tend to decrease markedly the measured intensity. This distance was set such that a secondary diffraction fringe was accidentally discounted. Another question might arise from apparent fringes in the ESRF graph of the harmonic rings. There are fringes (as is plainly visible in our graph) but the actual scale of apparent fringes in the ESRF graph is

almost certainly due to pixellation in their graph, and is not a real effect.

Conclusions

In this paper we obtained both an integral form for measurements of undulator radiation, and a very accurate approximation to this integral using Anger and Weber functions. We also compared profiles obtained using these forms to those that could be found elsewhere, and we compared the forms to each other as well.

Our results were based upon the assumption of a filament electron beam. While this is an ideal case, it is not completely accurate, and evaluations of the undulator radiation for beams with finite electron spread (using these general forms) should be completed. In addition, an evaluation of the errors that come from approximations in developing the integral form (small θ and ψ , for example) should be completed. A complete check of the accuracy of the analytic form with respect to the integral should be made when the value of η is not an integer (i.e. when the radiation is not on a harmonic), if this is possible. In addition, comparisons between our calculations and actual measurements of radiation from an undulator are much to be desired.

Acknowledgments

I would like to acknowledge Richard Talman, of Cornell University, who proposed this research project and worked extensively with me in its completion. I would also like to thank Richard Galik and Gerald Dugan, also of Cornell University, who obtained the REU grant that allowed me to come to Cornell and were available for questions about the program after my arrival.

This work was supported by the National Science Foundation REU grant PHY-0097595 and research grant PHY-9809799.

Footnotes and References

1. A. Hofmann, *Characteristics of Synchrotron Radiation*, in CERN Accelerator School 98-04, 1998.
2. K. Kim, *Characteristics of Synchrotron Radiation*, in Physics of Particle Accelerators, M. Month and M. Dienes, editors, AIP 184, 1988.
3. R. Talman, *The Storage Ring as Radiation Source*, 2001.
4. R. Talman and L. Kotredes, *An Explicit Formula for Undulator Radiation*, 2001.
5. G. N. Watson, *A Treatise on the Theory of Bessel Functions*, 2nd Ed. Cambridge, 1958.